M&C 2017 - International Conference on Mathematics & Computational Methods Applied to Nuclear Science & Engineering, Jeju, Korea, April 16-20, 2017, on USB (2017)

Reactor Core Simulations for Determination of the Antineutrino Spectrum for the SoLid Experiment at BR2 Reactor

Silva Kalcheva, Geert Van den Branden, Vadim Kuzminov and Edgar Koonen

SCK•CEN, Boeretang 200, Mol, 2400, Belgium, skaltche@sckcen.be

Lydie Giot and Muriel Fallot

SUBATECH, Ecole des Mines de Nantes - CNRS/IN2P3 - Université de Nantes, 4 rue Alfred Kastler, 44307 Nantes Cedex 3 – France

On behalf of the SoLid collaboration:
Universiteit Antwerpen, Vrije Universiteit Brussel. University of Bristol, Universiteit Gent, LAL Orsay, LPC Clermont-Ferrand Caen, Imperial College London, University of Oxford, SCK•CEN Mol, Subatech Nantes and Virginia Tech

Abstract - *Large quantities of antineutrinos are produced in a reactor due to beta decays of the fission products. The detection of these antineutrinos associated to reactor simulations could provide a method to assess both the thermal power and the evolution of the core fuel composition. One of the aims of the SoLid experiment located at the BR2 research reactor (SCK•CEN, Mol) is to investigate the ability of reactor monitoring with an antineutrino detector based on ^{6}Li scintillator and the use of such a detector for safeguards purpose. A detailed simulation of the BR2 reactor is needed to calculate the antineutrino spectrum emitted by the core for each cycle, i.e. for a given fuel loading map and operation history. A detailed MCNPX/CINDER90 3-D simulation of the fission rates distribution in the BR2 core will be coupled with the MURE (MCNP Utility for Reactor Evolution) code. The MCNP methodologies for the calculation of the emitted antineutrino spectrum and reactor core simulation are discussed. The results of first antineutrino rate prediction for the BR2 operation cycle 01/2015A are presented.*

I. INTRODUCTION

In recent years an increase interest has been drawn toward short baseline experiments for antineutrino detection. Such experiments require high neutron flux and opportunity for installation of the antineutrino detector close to the reactor core and at low backgrounds at the same time. The BR2 research reactor in the Belgian Nuclear Research Centre (SCK•CEN) in Mol, Belgium, driven by HEU fuel in a very compact core is an intense source of antineutrinos $\overline{\nu}_e$, providing about 1.0 x 10^{19} $\overline{\nu}_e$/s at nominal power 60 MW.

The SoLid experiment, installed at ~ 5.5 m from the BR2 reactor core, aims to validate a new technology to consolidate the use of antineutrinos as a safeguard tool with a detector using a composite scintillator (~ 3 tons) based on ^{6}Li [1]. The detection of these antineutrinos associated to reactor simulations could provide a method to assess both the thermal power and the evolution of the core fuel composition [2,3]. Another goal of the experiment along with many other short baseline oscillation experiments going on worldwide is to search for the existence of sterile neutrinos [4].

A key ingredient in the success of the SoLid experiment is the accurate calculation of the antineutrino spectrum emitted by the core. A detailed simulation of the BR2 reactor is needed to calculate the antineutrino spectrum emitted by the core for each cycle, i.e. for a given fuel loading map and operation history. A detailed MCNPX/CINDER90 3-D simulation of the fission rates distribution in the BR2 core will be coupled with the MURE code. The Monte-Carlo depletion code: MURE (MCNP Utility for Reactor Evolution) has been developed in order to compute the antineutrino energy spectrum emitted by a PWR reactor but also by research reactors [5]. In this paper, the MURE code and the on-going developments for the BR2 simulation will be presented. The methodologies for the calculation of the emitted antineutrino spectrum and reactor core simulation will be discussed. The results of first antineutrino rate prediction for the BR2 operation cycle 01/2015A will be presented.

II. THE SOLID EXPERIMENT

The SoLid experiment aims to provide a significant contribution to the ability of reactor monitoring via a new approach using a highly segmented detector based on Lithium-6. The SoLid technology for antineutrino detection is innovative compared to the classical approach based on liquid scintillator which generates problems related to safety, compactness and sensitivity to backgrounds [1]. The SoLid detector (Fig. 1) is a segmented detector (2.88 t.) divided in 10 modules (1.2m x 1.2m x 0.2m). Each module consists of 4 planes of 576 plastic scintillation

PolyVinylToluene (PVT) cubes of size of (5×5×5) cm^3, each cube being covered with one layer highly sensitive to thermal neutrons (^{6}LiF:ZnS(Ag)). Antineutrino interacts with protons in the PVT cubes through the inverse beta-decay process with threshold energy of 1.8 MeV producing a neutron and a positron:

$$\bar{\nu}_e + p \rightarrow e^+ + n. \qquad (1a)$$

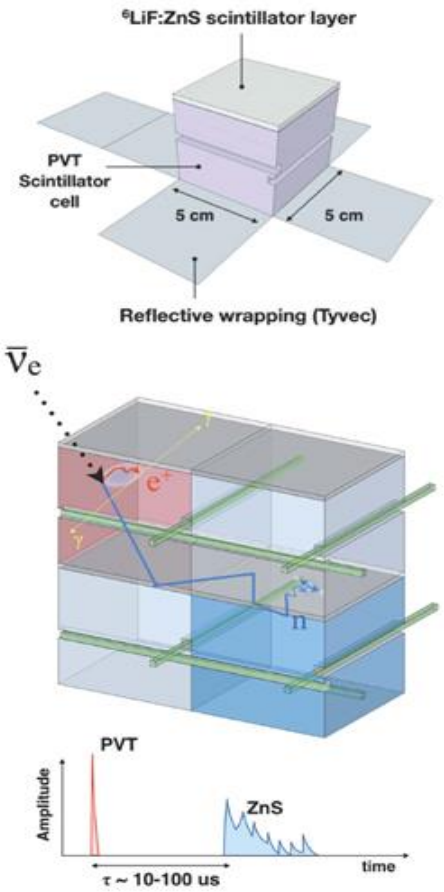

Fig. 1. Inverse Beta Decay interactions in the SoLid detector: (top) Schematic of the detector element: the PVT cube is covered with a layer of ^{6}LiF:ZnS(Ag) which are together wrapped in a reflective material. (center) Principle of the $\bar{\nu}_e$ detection in a volume made of separated voxels. The wavelength shifting fibers placed in perpendicular orientations are used to collect the scintillation light from each voxel (PVT and ZnS) of the array. (bottom) Corresponding scintillation decay and coincidence times used to identify the products of the $\bar{\nu}_e$ interaction.

A neutrino event is then defined by the time coincidence detection of a neutron and a positron. The coincidence time is determined by the neutron reaching thermalization and capture time on the Lithium-6 atoms present on the face of the cubes. The outgoing neutron thermalizes after a few elastic scatters and is eventually absorbed in the layer rich in Lithium-6 through the reaction:

$$n + {}^6Li \rightarrow {}^3H + \alpha + 4.78\,\text{MeV}, \qquad (1b)$$

which produce scintillation in the Ag-doped ZnS scintillator. Due to the high absorption cross section of ^{6}Li, only a small fraction of neutrons (~10%) will be captured by the hydrogen in the PVT cube. The outgoing nuclei have sufficient kinetic energy to escape a few tens of microns in the mixture and excite the inorganic scintillator (ZnS). ZnS has a de-excitation time that is significantly longer for neutron capture than for low energy density signals, i.e. tens of microseconds compared to tens of nanoseconds (see the bottom in Fig. 1). The IBD reaction products (see Eq. 1a) can thus be distinguished using the pulse shape information and the time difference between the positron and the neutron induced signals.

The antineutrino energy spectrum emitted by the BR2 core will be calculated for each cycle, i.e. for a given fuel loading map and operation history and provided as a reference for the antineutrino detection to the SoLid experiment.

III. METHODOLOGIES USED FOR CALCULATION OF EMITTED ANTINEUTRINO SPECTRUM

Two basic methods are used for the calculation of the antineutrino spectrum. The first method uses automatic coupling of the MCNP code with the 1-D depletion code CINDER90 (included in latest versions of MCNPX [6] and MCNP6 [7]). This method takes advantage of the important simulation work already done at SCK•CEN [8,9] coupled with data processing tools developed with PYTHON [10] for a quick access to a first antineutrino calculation. The second method developed at SUBATECH uses an adapted version of the code MURE for the computation of the antineutrino spectrum.

1. BR2 Reactor Core Evolution Simulation with MCNP

A. Description of the BR2 Reactor

The Belgian Material Test reactor (MTR) BR2 is a strongly heterogeneous high flux engineering test reactor operated by SCK•CEN at the Mol site in Belgium. This tank-in-pool reactor is cooled by light water in a compact HEU core (93% ^{235}U), positioned in and reflected by a beryllium matrix. The beryllium matrix is an assembly of a large number of irregular hexagonal prisms which are skew and form a twisted hyperbolic bundle around the central 200 mm channel H1. The reactor is presently operated at the power level of 50÷100 MW, currently 130 to 150 full power days per year with thermal neutron flux 1.2×10^{15} $cm^{-2}.s^{-1}$ and fast neutron flux 1.0×10^{15} $cm^{-2}.s^{-1}$ at power 60 MW.

B. 3-D Geometry Model of the BR2 Reactor

A 3-D geometry and burn-up model of the BR2 core has been developed by the SCK•CEN team using the latest versions of the Monte Carlo transport code MCNP [6,7]. The model is a complete 3-D description of BR2's one sheet hyperboloid reactor core composed of twisted and inclined reactor channels and represents each channel separately, with its individual position and inclination (see Fig. 2). The fuel assemblies, beryllium plugs, experimental devices and control rods loaded in the channels are modeled with the same level of details. The fuel region of each of the 6 fuel rings of every fuel element is axially divided into 10 material cells of 6 cm height and 2 extreme cells of 8.1 cm height.

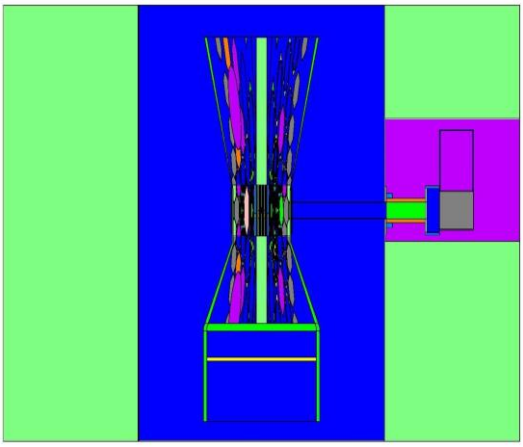

Fig. 2. MCNP model of the BR2 reactor including the vessel and the bio shield.

C. MCNP Methodology

The MCNPX or MCNP6 simulation is coupled for the evolution part with CINDER90, which is included in either code. The credibility of the MCNPX model was demonstrated by multiple comparisons of code predictions with available experimental data, such as control rod worth's, neutron fluxes, gamma heating, linear power and fission rates, reactivity effects, etc. [8,9] (see also further chapter IV).

The preferred approach for the whole core automatic depletion calculations is to take advantage of the existing symmetries of the burned fuel material distribution in the core, i.e., the axial, radial and azimuth symmetries around the core center, in order to significantly reduce the computation time. In this case it is not necessary to give a unique material number to each burn-up cell. Cells having similar burn-up and power will experience the same composition evolution and can therefore be given the same material number. The MCNP model developed for this approach has a total of 2304 burn-up cells (12 axial zones x 6 fuel rings x 32 fuel elements + 16 beryllium matrix regions) with 56 unique materials (40 materials for the fuel and 16 materials for the beryllium matrix). Increasing the number of unique burn up materials improves in general the accuracy of whole core criticality calculations. In this case MCNPX/MCNP6 burns each unique material at the specific flux in the spatial cell, occupied by the material, generating automatically unique spatial flux solutions and unique spatial fuel compositions. However, burning a unique material will increase the statistical uncertainty in power/depletion determination due to the reduced calculation volume of the unique burn up cell. Therefore, a compromise between the used NPS per depletion step and the number of unique burn up materials was made based on the existing symmetries of the burned fuel material distribution in the core as described above.

2. Antineutrino Spectrum Calculations and Reactor Simulations with MURE

A. Neutrino Flux Calculation

Large quantities of antineutrinos are produced in a reactor due to beta decays of the fission products. The detection of these antineutrinos associated to reactor simulations could provide a method to assess both the thermal power and the evolution of the core fuel composition. The number of emitted antineutrinos produced in a reactor core over the time t_{run} is defined by [11]:

$$N_{\bar{\nu}}(E) = \int_0^{t_{run}} \frac{P(t)}{\Sigma_k . \alpha_k(t) . E_k} \sum_k \alpha_k(t) . S_k(E) dt. \quad (2)$$

The first term of the equation, accounting for the number of fissions occurring over the time, is the ratio of the thermal power (provided by the operators through measurements) over the average energy released per fission of the 4 isotopes (^{235}U, ^{238}U, ^{239}Pu and ^{241}Pu) present in the fuel. $\alpha_k(t)$ stands for the percentage of fissions undergone by the isotope k. The mean energy released per fission by each fissile isotope E_k is stored in nuclear databases. The second term represents the total antineutrino spectrum emitted by a reactor per fission. It is defined as the sum over the 4 isotopes of the fraction of fissions undergone by the k^{th} isotope times the antineutrino spectrum per fission of the same isotope $S_k(E)$ which can be calculated either using the conversion method or the summation method [5,11-13].

B. The Conversion Method

The conversion method [12,13] is based on the measured β^- - spectra of a fissile isotope at a given irradiation time and then is converted to $\overline{\nu_e}$. The conversion

procedure consists from two steps. First, the fission rates of the primary fissile isotopes are calculated, usually ^{235,238}U and ^{239,241}Pu. Then, the weighted sums of the fission rates for the four fissile isotopes are convolved with the antineutrino spectrum, the sum of the spectra from the β^- - decay of each isotope's fission products. To be converted to a neutrino spectrum, each measured β^- - spectrum must be fitted by a set of branches [12-14].

For ^{235}U and ^{239,241}Pu, the only β^- - spectra available are those from the ILL research reactor [15-18], which were acquired after a quite short irradiation time in a quasi-pure thermal neutron flux, between 12 hours and 1.8 days depending on the isotopes. For antineutrino experiments, the irradiation time will be longer. Among the fission products, about 10% of them have a β^- - decay life-time long enough to keep accumulating after several days. The increase in the flux caused by the decay of these long-lived fission products has to be taken into account in the flux calculation with the conversion method, known as off equilibrium corrections.

C. The Summation Method

The summation method computes the $\overline{\nu_e}$ spectrum emitted from a fissile isotope: ^{235,238}U and ^{239,241}Pu but also other actinides produced during the operation cycle as the sum of all contributions of the beta decay branches of its fission products using the full information available per nucleus in nuclear databases [11]. This method allows also to compute the off equilibrium corrections (due to the build-up of long lived fission products, and to neutron captures on fission products during the core cycle) to be applied to the conversion method. In addition, the summation method is the only one allowing to predict antineutrino spectra associated to innovative fuels or reactor designs. This method is thus indispensable in the context of the study of proliferation scenarios with antineutrino detection.

The antineutrino energy spectra in this method can be computed in two different ways. In the first case, the complete core model is used to provide the amount in-core of all β^- - emitters, allowing for the first time to take into account all the contributions, i.e. not only the fission products but also the contribution of the actinides and heavy nuclei produced during core operation. The $\beta^-/\overline{\nu}$ energy spectrum emitted by the reactor core is thus broken-up into the sum of all $\beta^-/\overline{\nu}$ spectra of the β^- - emitters (labelled *be*) in-core, weighted by their activity A_{be}:

$$S(E,t)=\sum_{be=1}^{N_{be}} A_{be}(t)\times S_{be}(t) \qquad (3)$$

The $\beta^-/\overline{\nu}$ spectrum of one β^- - emitter is the sum over the *b* branches of all β^- - decay spectra (or associated $\overline{\nu}$ spectra), S_{be}^{b} (in Eq. 3) of the parent nucleus to the daughter nucleus is weighted by their respective branching ratios as

$$S_{be}(E)=\sum_{b=1}^{N_b} BR_{be}^{b}(t)\times S_{be}^{b}\left(Z_{be}, A_{be}, E_{0be}^{b}, E\right) \qquad (4)$$

In the second case, the complete core model is only used to provide the fission rates, which are then weighted with individual uranium and plutonium isotope spectra computed with the summation method, to obtain the total spectrum emitted by the BR2 reactor. This method is similar to the one used by reactor neutrino experiments i.e. weight of individual antineutrino spectra from the main uranium and plutonium isotopes with their fission rates (see Eq. 2). In this paper, the $\beta^-/\overline{\nu}$ spectrum per fission of a fissile isotope $S_k(E)$ is calculated with the summation method, i.e. it is the sum of all fission product $\beta^-/\overline{\nu}$ spectra weighted by their activity A_{fp},

$$S_k(E)=\sum_{fp=1}^{N_{fp}} A_{fp}\times S_{fp}(E) \qquad (5)$$

where $S_{fp}(E)$ is computed as in Eq. 4.

D. The MURE Code

The code MURE is coupled to nuclear databases containing all beta decay branches of the fission products for a given fissile isotope. In the framework of several antineutrino experiments [5,19] SUBATECH has developed important new functions in MURE to analyze the beta decay properties of the fission products in order to compute the associated antineutrino energy spectrum together with the reactor core evolution simulation. Available at the NEA databank, the MURE (MCNP Utility for Reactor Evolution) code is a precision, open-source code, designed by CNRS/IN2P3 laboratories and written in C++ which automates the preparation, computation of successive MCNP (Monte Carlo N-Particle) calculations and solves the Bateman equations in between, using a Runge-Kutta method, for burnup purpose [20]. The MURE code is highly flexible to simulate reactors with a variety of refueling schemes, operation history and non-trivial core geometry [21].

The principle of the evolution calculations is similar to that in MCNPX/MCNP6 (see Fig. 3). It calculates the fission fractions as a function of the reactor history and allows following up as a function of time all the fission products, which are needed for the summation method. The quality of the MURE simulations has been evaluated through various benchmarks, such as the Takahama benchmark [22]. MURE inventories of two assembly types used in the Chooz reactors were compared to those obtained with the DRAGON code and the APOLLO-2F code [19].

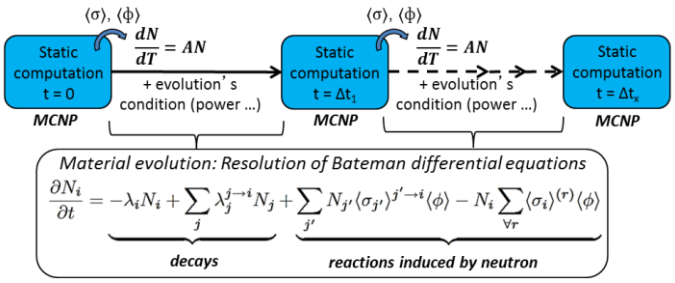

Fig. 3. Scheme of MURE code evolution calculation: same as MCNPX/MCNP6.

IV. VALIDATION OF THE MCNP METHODOLOGY

The validation is performed using experimental data and cross-code comparison. The MCNP methodology has been verified on various experimental data, including routine measurements of critical heights of control rods motion during each operating cycle, measurements of control rod worth, reactivity effects of experiments (e.g. various contents of H1 and H1/Central channels, PRF loading/unloading effects, etc.), on dosimetry measurements of neutron fluxes in CALLISTO loop, aluminum vessel; on measurements of isotope activities; on measurements of gamma heating and linear power in MOX fuel rods.

1. Critical Height

The most straight-forward way to evaluate the results of the core load management calculations using the MCNP-based method is comparison of the predicted and measured value for the critical height whenever a reactor load is assembled.

Table I shows the critical height of a sample of different reactor loads assembled during measurement campaigns and/or in preparation of a suitable load for a reactor cycle at nominal power. The measured critical heights as well as the predicted critical height by MCNP are listed. As can be seen in this table, the corresponding reactivity difference between the two critical heights remains limited.

2. Reactivity Evolution During a Reactor Cycle

The calculation of the evolution of the reactivity for the reactor core load management as a function of produced energy is one of the main results of the reactor core simulations. It, firstly, permits to evaluate the minimum available negative reactivity (safety margin) at any moment of the cycle as prescribed by the Technical Specifications to be respected. Secondly, it permits to evaluate operational parameters like, the maximum cycle length and the reactivity effect of the ^{135}Xe – ^{149}Sm-transient at the start-up of the reactor. This last value can be important for some cycles. If the control rods would need to be raised above 900 mm (which corresponds to fully withdrawn control rods) at the start of the reactor to overcome the effect of the combined ^{135}Xe cannot be started. Third, the correct evaluation of the reactivity evolution during the operation cycle is an indirect indication for the accuracy of the fuel burn-up modeling.

Figure A.1 to Figure A.4 in Appendix A show the evolution of the reactivity of the BR2 reactor as a function of produced energy for the cycles of the years 2012 till 2015 as measured and as predicted by the MCNP-based simulations.

Table I. Comparison of the critical heights of a sample of different BR2 reactor loads, see Ref. [22].

BR2 operation Cycle #	Critical height Sh_{crit} Predicted by MCNP [mm]	Critical height Sh_{crit} Measured [mm]	Reactivity difference Δρ Measured – Predicted [pcm]
01/2011.A3	610	617	-108
06/2010.A2	468	453	+317
06/2010.A4	465	471	-130
05/2010.A2	570	555	+266
05/2010.A3	555	547	-144
04/2010.A4	456	456	0
03/2010.M6	465	442	+410
03/2010.M7	455	460	-86
Average deviation (sum of absolute values)			≈200

To quantify the differences between the reactivity evolution ρ_{MCNP} predicted by MCNP and the measured reactivity evolution ρ_{meas}, six evaluation indicators have been defined:

$$\Delta_{max} = \max \left| \rho_{MCNP} - \rho_{meas} \right|, \qquad (6)$$

the maximum difference between both reactivity evolutions[11],

$$\Delta_{average} = \frac{\int_0^{E_{produced}} dE\left(\rho_{MCNP} - \rho_{meas}\right)}{E_{produced}}, \qquad (7)$$

[1] If the maximum of $\left|\rho_{MCNP} - \rho_{meas}\right|$ occurs for $\rho_{MCNP} < \rho_{meas}$, Δ_{max} gets a negative sign. If the maximum of $\left|\rho_{MCNP} - \rho_{meas}\right|$ occurs for $\rho_{MCNP} > \rho_{meas}$, Δ_{max} gets a positive sign.

$$\Delta_{|average|} = \frac{\int_0^{E_{produced}} dE\left|\rho_{MCNP} - \rho_{meas}\right|}{E_{produced}}, \quad (8)$$

$$\Delta_{\text{at minimum}} = \rho_{\text{MCNP}}(\text{at min.}) - \rho_{\text{meas}}(\text{at min.}), \quad (9)$$

$$\Delta_{\text{at Xe peak}} = \rho_{\text{MCNP}}(\text{at Xe peak}) - \rho_{\text{meas}}(\text{at Xe peak}), \quad (10)$$

$$\Delta_{\text{at EOC}} = \rho_{\text{MCNP}}(\text{at EOC}) - \rho_{\text{meas}}(\text{at EOC}). \quad (11)$$

The first three indicators, Δ_{max}, $\Delta_{average}$, $\Delta_{|average|}$ give an overall evaluation of the difference between the two reactivity evolutions. The last three indicators, $\Delta_{\text{at minimum}}$, $\Delta_{\text{at Xe peak}}$, $\Delta_{\text{at EOC}}$ give a detailed evaluation of three key moments in the reactor cycle: at the minimum of the rods (important for safety), at the ^{135}Xe –^{149}Sm peak (important for the start-up) and at the End Of Cycle (EOC, important for the cycle duration). Figure 4 gives a graphical representation of the indicators listed above for a '***fictive***' reactor cycle. The results of the indicators for the reactor cycles of the years 2012 till 2015 are listed in Table II.

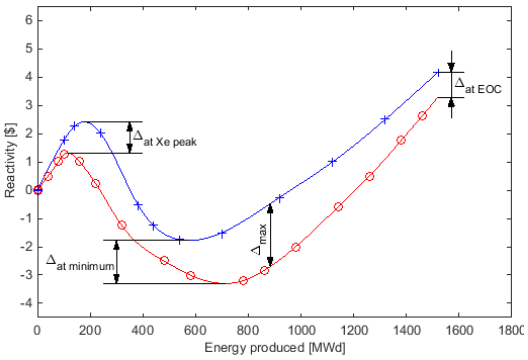

Figure 4. ***"Fictive"*** evolution of the reactivity of the BR2 reactor as a function of produced energy: as measured (blue), as predicted by the MCNP based simulations (red). The definitions of the evaluation indicators as reported in Table II are depicted. ***The differences between the 'fictive' measured and calculated values in Figure 4 are exaggerated only to better illustrate the meaning of the indicators (see the real graphs in Appendix A)***

Table II. Evaluation indicators of the reactivity evolution as a function of produced energy of the MCNP based predictions compared to the measured evolution for cycles 01/2012 to 01/2015, see Figure A.1 to Figure A.4 in Appendix A.

year	cycle	Δ_{max} [$]	$\Delta_{average}$ [$]	$\Delta_{\lvert average\rvert}$ [$]	$\Delta_{\text{at minimum}}$ [$]	$\Delta_{\text{at Xe peak}}$ [$]	$\Delta_{\text{at EOC}}$ [$]
2012	1	0.34	-0.11	0.13	-0.02	0.05	-0.05
2012	2	1.27	0.32	0.34	0.17	-0.15	1.27
2012	3	0.79	0.63	0.64	0.72	0.23	0.73
2012	4	0.42	0.20	0.22	0.39	0.24	0.06
2012	5	-0.51	-0.28	0.29	-0.50	-0.02	0.23
2013	1	0.63	0.10	0.11	0.07	0.47	0.33
2013	2	-1.00	-0.43	0.48	-0.06	-0.09	0.09
2013	3	-0.55	-0.33	0.33	0.01	0.10	-0.08
2013	4	0.41	0.02	0.11	0.13	0.10	0.27
2013	5	-0.53	0.03	0.11	0.04	-0.09	0.53
2013	6	0.44	0.09	0.19	0.33	0.38	0.40
2014	1	1.41	-0.09	0.50	-0.11	0.23	1.36
2014	2	-0.72	-0.44	0.45	-0.05	-0.11	-0.38
2014	3	-0.89	-0.47	0.50	-0.37	0.06	0.28
2014	*4*[2]	*2.29*	*1.60*	*1.60*	*2.19*	*0.38*	*1.01*
2014	5	0.96	0.48	0.49	0.34	0.06	0.96
2014	6	0.68	0.15	0.17	0.20	0.01	0.68
2015	1	0.98	0.52	0.52	0.49	0.38	0.98
range	$\min\{\Delta\}$	-1.00	-0.47	0.11	-0.50	-0.15	-0.38
	$\max\{\Delta\}$	1.41	0.63	0.64	0.72	0.47	1.36
mean	$\overline{\Delta}$	0.24± 0.78	0.02± 0.34	0.33±0 .18	0.11± 0.30	0.11± 0.19	0.45± 0.49
	$\overline{\lvert\Delta\rvert}$	0.74± 0.31	0.28± 0.19	0.33±0 .18	0.24± 0.21	0.16± 0.14	0.51± 0.42

Figure A.1 to Figure A.4 in Appendix A and the results listed in Table II for the different indicators show that the difference between values predicted by the MCNP-based method and measured values remains limited. Since predicting the reactivity evolution as a function of energy produced involves several iterative operations in a detailed three-dimensional mesh model (in total about 2500 fuel and beryllium burn-up meshes):

- spatial flux distribution calculations over the whole reactor core,
- reaction rates calculations in hundreds of material zones (fuel, beryllium, experiments, ...)

[2] Cycle 04/2014 was not taken into account for the calculation of the range and mean of the evaluation indicators, since due to the large non-adequate value of the control rod bank reactivity worth used for the measured reactivity evolution the results are not representative for the evaluation.

• burn-up calculations for all these material zones,

making a good prediction of the reactivity curve implicitly[3] means that all these different operations had to be performed adequately.

3. Burn-up Determination

The burn-up determination based on MCNP calculations is firstly evaluated by comparison with results of burn-up measurements for three sets of fuel irradiation experiments[4] performed in the BR2 reactor. Two different experimental burn-up measurement methods, viz. γ – spectrometry and radiochemistry, have been used.

A. MCNP vs. γ - Spectrometry

The first fuel irradiation burn-up evaluation is based on results from an irradiation program[5] whereby the fission density of three fuel plates was determined using MCNP calculation results as well as measured by γ – spectrometry. The results for these fission densities are listed in Table III. As can be seen from this table the results correspond very well. The maximum difference is < 5%.

Table III. Mean fission density of three fuel plates as determined based on MCNP calculations and as measured by γ – spectrometry.

Method	Mean fission density [fissions/cm³]		
	Plate 1	Plate 2	Plate 3
MCNP based	3.38×10^{21}	4.98×10^{21}	4.89×10^{21}
γ-spectrometry	3.51×10^{21}	5.12×10^{21}	5.10×10^{21}
Difference [%]	3.8	2.8	4.3

[3] For the calculation of the burn-up with the MCNP-based method, also a more explicit evaluation is reported in further Section 3.

[4] The burn-up of standard fuel elements is not measured directly on a routine basis. It can be determined indirectly by comparison between the measured reactivity effects and the reactivity effects calculated by the MCNP-method.

[5] The reports of this irradiation program have a restricted status, therefore, no further details of this program can be provided.

B. MCNP vs. Radiochemistry

The second fuel irradiation burn-up evaluation is based on results from an irradiation program[6] whereby the Fissions per Initial Metal Atom (FIMA) of a fuel plate was determined using MCNP calculation results as well as measured by radiochemistry. The results for these fission densities are listed in Table IV. As can be seen from this table the results again correspond very well. The maximum difference is < 5%.

The small differences between the calculated and measured values of the burn-up as reported in Table III and Table IV show that the MCNP based calculations are capable of determining fuel burn-up in the BR2 reactor.

Table IV. Fissions per Initial Metal Atom (FIMA) of a fuel plate as determined based on MCNPX calculations and as measured by radiochemistry (see supra 5).

Method	FIMA [%]
MCNP based	11.2
Radiochemistry	10.68
Difference [%]	4.8

C. MCNP & On-Line Thermal Balance Measurement vs. γ - Spectrometry

The third direct fuel irradiation burn-up evaluation is based on the comparison of the combination of on-line thermal balance measurement and MCNP-based calculations versus γ-spectrometry measurements for the GERONIMO fuel irradiation campaign, see Ref. [23] and Ref. [24]. During this campaign fuel irradiation transient tests have been performed for MOX fuel rod in the PWC/CCD device loaded in BR2 reactor channel. The activity of certain isotopes of suitable half-life (e.g. ^{140}Ba, ^{140}La) can be measured by γ-spectrometry and, taking into account the appropriate factors, be converted into linear power, see Ref. [24]. Table V presents the results of these comparison for four fuel rods irradiated in the PWC/CCD device during the GERONIMO fuel irradiation campaign, see Ref. [23] and Ref. [24].

[6] See supra 5.

Table V. Comparison of the on-line power determination (based on combination of thermal balance measurements and MCNP-calculations) with the γ-spectrometry measurements, see Ref. [23] and Ref. [24].

Fuel rod	BR2 power	Fission rate	Total fuel power	Average linear fuel power after the transient		
		Measured by γ-spectro metry	Measured on-line by thermal balance & MCNP	Measured by γ-spectro metry	Measured on-line by thermal balance & MCNP	Diffe rence
	[MW]	[s^{-1}]	[W]	[W/cm]	[W/cm]	[%]
1	14.0	3.924×10^{14}	12510	301.3	297	+1.4
2	20.5	5.797×10^{14}	18482	446.3	425	+4.8
3	20.7	5.537×10^{14}	17653	423.5	426	-0.6
4	16.6	5.068×10^{14}	16158	388.7	369	+5.1

D. Reactivity Effects of Fuel Elements with Different Burn-Up

Next to the first evaluation of the burn-up determination performance of the MCNP-based method, viz. by comparison with three series of experimental burn-up measurements using γ spectrometry or radiochemistry, the evaluation of the burn-up can be performed indirectly by comparison of the reactivity effect of loading fuel elements with various burn-up in the same BR2 reactor channel as measured and as calculated by MCNP. Only if the burn-up is modelled correctly, the measured and calculated reactivity effects will correspond.

In the framework of the conversion of the BR2 reactor from HEU to LEU fuel system, an irradiation campaign was performed with two HEU fuel elements not having the standard burnable poisons in the fuel meat (B_4C and Sm_2O_3) but instead having burnable poisons in the stiffeners (cadmium wires), see Ref. [25] and Figure 5.

The two fuel elements with cadmium stiffeners were irradiated for 5 reactor cycles and the reactivity effect of the burn-up of the fuel element was measured experimentally. These results were compared with the calculated reactivity effects with the MCNP-based method, see Ref. [25]. Figure 6 shows the results of this comparison. The evolutions of the reactivity vs. the burn-up as measured experimentally and as calculated by the MCNP-based method correspond. The differences were somewhat larger at the end-of-life of the fuel element which was due to change of the foreseen surrounding conditions (N.B. The MCNP calculations were performed in advance to the measurement for slightly different surrounding conditions of the tested FE).

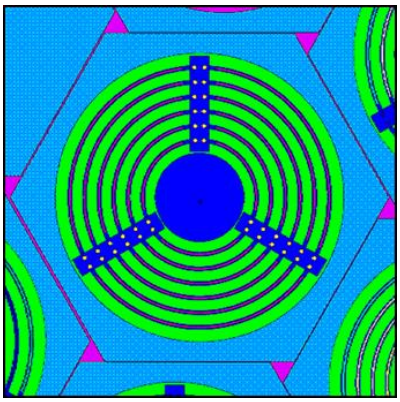

Figure 5. Cross-section of the MCNP model of a HEU fuel element with Cd wires as burnable absorber, see Ref. [25].

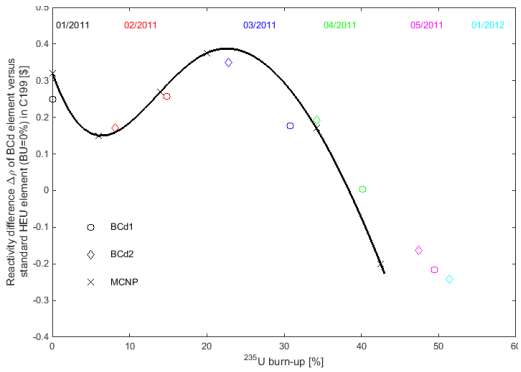

Figure 6. Reactivity effects as a function of burn-up of a HEU fuel element with cadmium wires as burnable absorber, see Ref. [25].

4. Comparison with Dosimetry Results

For thermal flux dosimetry, measurements have been made during cycle 02/2001.A using ^{59}Co foils, see Ref. [26]. The central reactor channel H1 and two more peripherally situated reactor channels, viz. G60 and G300, were monitored. Figure 7 and Figure 8 show the comparison between the measured and calculated values for the thermal neutron flux for the central channel H1 and for the peripheral channels G60 and G300, respectively. Figure 9 shows the axial distribution of the fission power as calculated and as measured (by γ- spectrometry) in the fuel plate located in channel G300. The measured and axial distributions are for each case in good agreement.

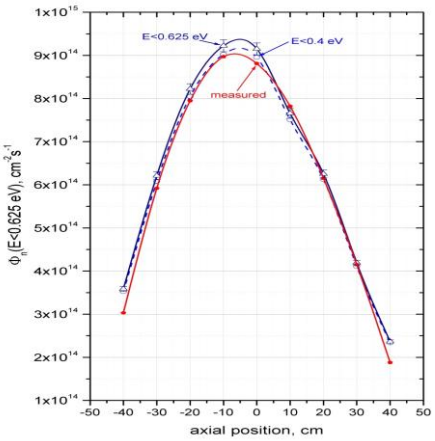

Figure 7. Axial distribution of the calculated and measured thermal flux in reactor channel H1 during cycle 02/2001.A, see Ref. [26].

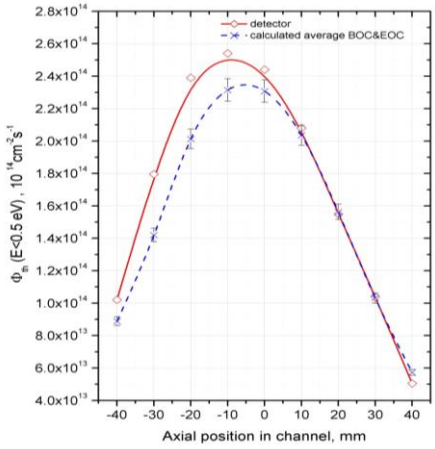

Figure 8. Axial distribution of the calculated and measured thermal flux in reactor channels G60 and G300 (the mean value of both channels is shown) during cycle 02/2001.A, see Ref. [26].

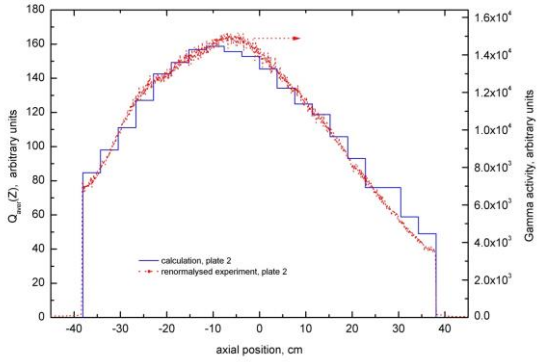

Figure 9. Axial distribution of the calculated and measured fission power for the fuel plate in channel G300 during cycle 02/2001.A, see Ref. [26].

A similar comparison for fast fluxes involves the irradiation of vessel steel specimens in IPS1 and IPS3 of the CALLISTO loop. The fission flux was measured experimentally by dosimetry in different irradiation positions and at different axial heights (in total 31 dosimeters were used), see Ref. [27]. Table A.I and Table A.II in Appendix A show the results of the fission fluxes measured experimentally and compared to the fission fluxes calculated by MCNP. The difference between the measured and predicted neutron fluxes was typically less than 10%.

5. Cross-code Comparison of Isotopic Fuel Densities

The calculated with MCNPX/CINDER90 time evolutions of fuel isotopes have been cross-checked with the ALEPH code, see Ref. [28]. The time evolutions of major fuel isotopic densities during continuous irradiation in an infinite BR2 lattice cell are compared in Fig. 10, which shows a good agreement between both codes.

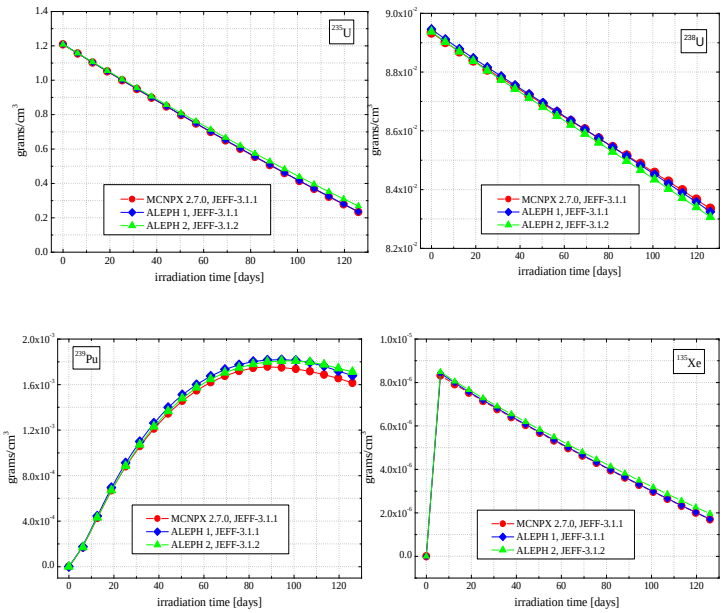

Fig. 10. Comparison of major fuel isotopic evolutions between MCNPX and ALEPH during continuous irradiation in an infinite lattice.

V. REACTOR SIMULATIONS FOR THE SOLID EXPERIMENT

The current strategy of the SoLid collaboration is to combine the work already performed by the SCK•CEN and SUBATECH. The BR2 team developed a 3-D model of the reactor with MCNPX (or MCNP6) which can be coupled to CINDER90 and used as a starting point to produce the fission rates. In addition to this highly segmented model, the MURE code will be used for the calculation of the emitted

antineutrino energy spectrum. Both codes will estimate and compare the off equilibrium corrections needed for the conversion method spectra. Summation method spectra will be also calculated from the fission products inventory obtained with MURE. In addition, comparative studies will be performed to estimate the systematic errors between both codes. Other systematic errors associated to these simulations (thermal power, temperatures, burnups, nuclear data…) will be also determined and propagated.

1. Fuel Assembly Benchmark

As a first step, a depletion benchmark was performed between the MURE code and MCNPX coupled to CINDER90 for a single fuel assembly in an infinite lattice in a hexagonal beryllium prism with a mirror boundary condition. Each of 6 fuel rings is embedded in an aluminum cladding, surrounded by water. The geometry produced with MURE is shown on Fig 11.

An irradiation time of 22 days is considered for the depletion calculation of this fresh fuel element (93% ^{235}U) with a constant power of 2 MW. The energies released per fission are taken from [29] for both codes. The input nuclear cross sections are respectively ENDF/B-VI.8 and ENDF/B-VII for the MURE and CINDER90 depletion calculations.

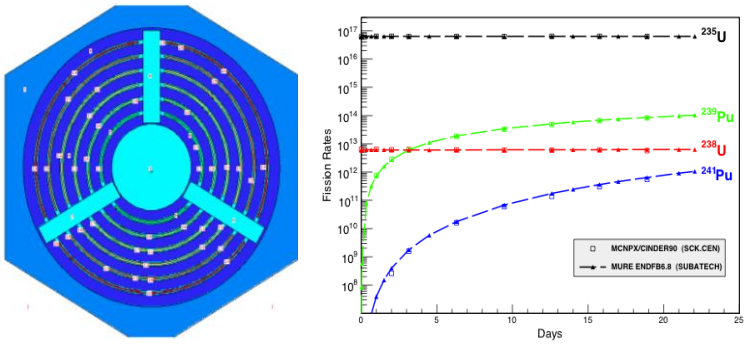

Fig. 11. Fuel element geometry produced with MURE (left); comparison of fission rates for a fuel cycle (right).

The instantaneous fission rates for ^{235}U, ^{238}U, ^{239}Pu and ^{241}Pu are shown on Fig. 11 as a function of time. The results are consistent between both codes. The fission rates are dominated by the contribution of the fission of ^{235}U (more than 99% due to the high enrichment of the fuel) and the difference between both codes range from -1.5% to 2.7 %.

2. Full Core Simulation

A. Cycle 01/2015A

The next step was to perform the full core simulation for a real BR2 operation cycle 01/2015A, which was operated from 27/01/2015 until 23/02/2015. To avoid the complete coding in a MURE format of the complex geometry of the BR2 core, the MCNP input file of the SCK•CEN team was externally read by MURE. For this purpose, an automatic MURE module was developed. The load map for this cycle is schematically presented in Fig. 12.

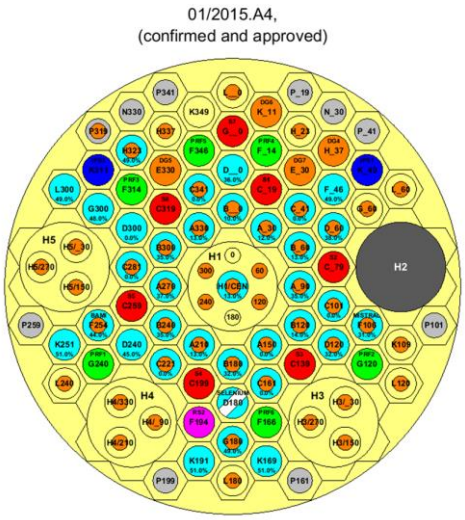

Fig. 12. Loading map for the cycle 01/2015A used for the calculation of the first antineutrino spectrum (blue color – fuel elements, red color – control rods, green & gray – irradiation experiments, yellow – beryllium matrix).

B. Power History

The precise predictions of the antineutrino spectra need important information from the reactor operation, such as the power history during the operation cycle. The detailed reactor power as function of the elapsed time is presented in Fig. 13.

Detailed study of the power history for depletion calculations was performed. The time steps for the reactor evolution were chosen to take into account the power variation but also the needs of the reactor calculation. In total 25 time steps have been chosen with fine discretization in the non-equilibrium xenon build-up regime (see Fig. 14).

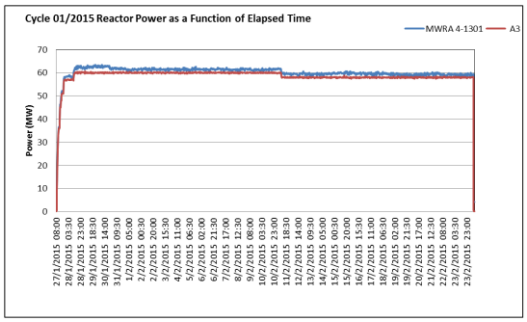

Fig. 13. Power history of Cycle 01/2015A, while module SM1 of the SoLid detector was recording data.

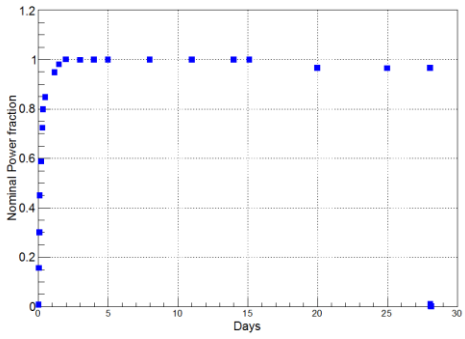

Fig. 14. Power history of Cycle 01/2015A, consisted of 25 time steps used for the depletion calculations by MCNP.

C. Energy Released per Fission

The fission energy released per fission in the HEU core of the BR2 reactor has been estimated using MCNP (see Ref. [29] and Table B.I in Appendix B for some details). The different components of the energy released per one fission event are summarized in Table VI. Using the data in Table VI, the recoverable fission energy for the Q-value in MCNPX, MCNP6 was adjusted in order to account for the actual distribution of the fission energy.

Table VI. Distribution of the fission energy in BR2.

Fission Energy	Deposited in Fuel Meat	Escaped from Fuel Meat
Fission	166.2 MeV	-
Beta particles,	7.0 MeV	-
Prompt γ	1.07 MeV	7.23 MeV
Delayed γ	0.66 MeV	6.64 MeV
Captured γ	-	5.20 MeV
Neutrons	-	4.8 MeV
TOTAL	174.93+23.87=198.8 MeV	

D. Development of Automatic Post-Processing Scripts for Calculation of Fuel Inventories and Fission Rates

PYTHON [10] has been used to process the output data from both MCNPX/CINDER90 and to extract at each time step the fuel inventories: fissile isotopes and fission products (see Fig. 15) and fission rates (Fig. 16).

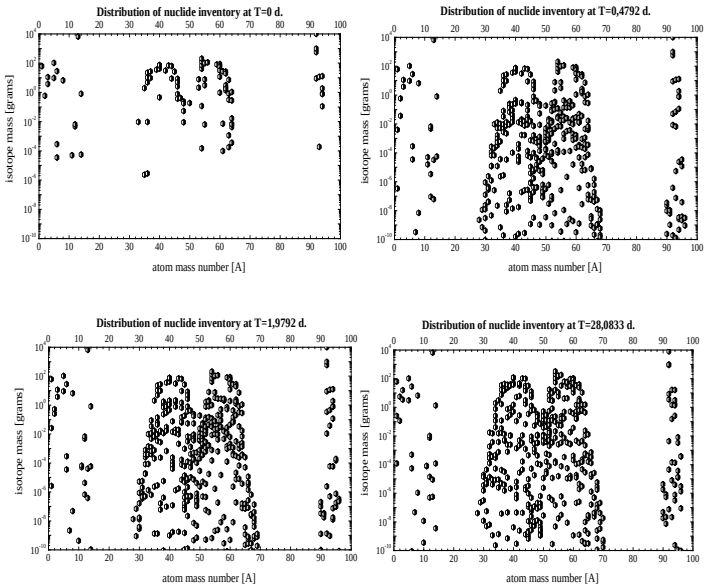

Fig. 15. Examples of fuel isotope inventories distributions during the irradiation cycle.

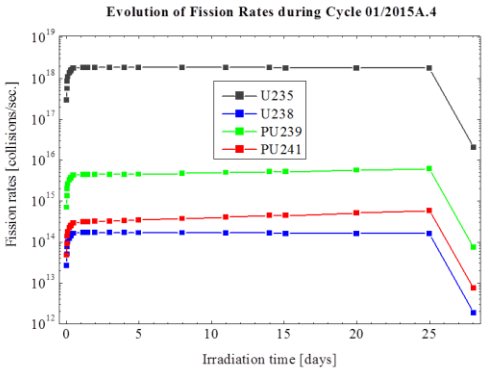

Fig. 16. Evolution of fission rates during Cycle 01/2015A.

E. First Antineutrino Spectrum

The emitted antineutrino flux and spectra during the cycle 01/2015A were computed with the fission rates calculated by MCNPX/CINDER90. Preliminary summation method spectra are given in the lower graph of Fig. 17.

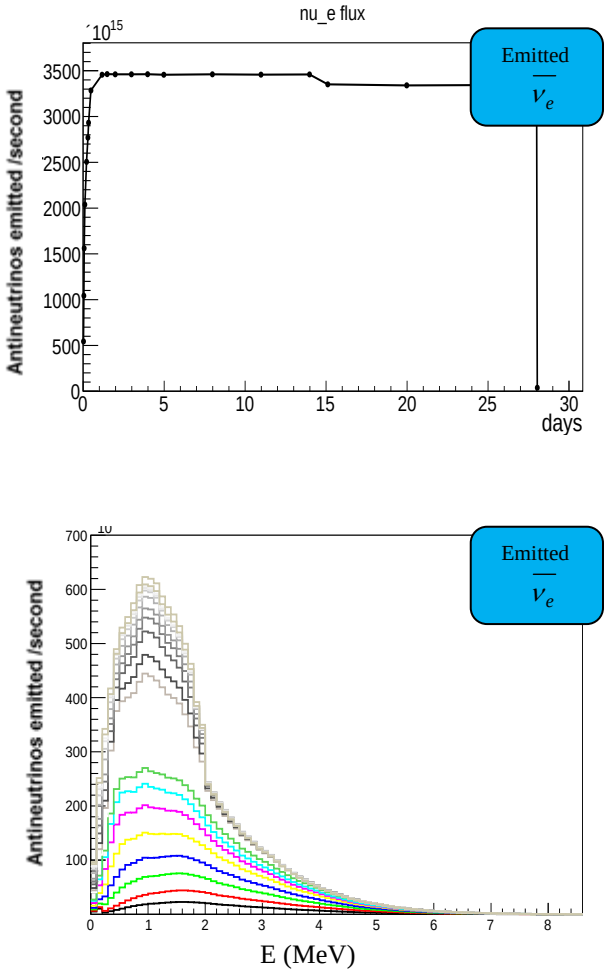

Fig. 17. Emitted antineutrino flux (upper graph) and spectrum (lower graph) calculated with MCNP fission rates and using the summation method (the different colors correspond to summations at different time steps).

The analysis of the data presented in Fig. 17 is important to study the impact of the different antineutrino emitters on the spectra in advance to compare/validate with future (pure) MURE simulation. After that the results for the fission rates and inventories as computed with MCNP are convolved with the Huber's antineutrino spectra converted from the measured ILL β^- - spectra from ^{235}U, ^{239}Pu and ^{241}Pu [14].

The emitted antineutrinos computed from the BR2 simulation with MCNP & MURE will be transmitted in the future to a GEANT4 simulation of the SoLid detector to obtain the real detected antineutrino rate by the detector. In the meantime, a first calculation of the detected antineutrinos was performed assuming 0.17% geometrical efficiency of the detector, surface exposure of 6400cm^2 and energy cut at 3.3 MeV, see Fig. 18.

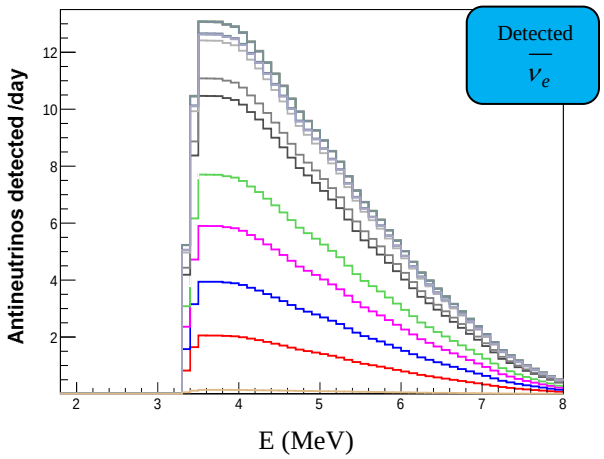

Fig. 18. Detected antineutrino spectrum (preliminary) calculated with MCNP/CINDER90 fission rates using the conversion method (the different colors correspond to summations at different time steps).

VI. CONCLUSIONS

The SoLid experiment, installed at SCK•CEN BR2 research reactor in Mol, aims to validate a new technology to consolidate the use of antineutrinos as a safeguard tool with a detector using a composite scintillator based on ^{6}Li. A key ingredient in the success of the experiment is the accurate calculation of the antineutrino spectrum emitted by the core. A first antineutrino rate prediction was presented using the conversion method: MCNPX/CINDER90 simulation for the complete reactor model coupled with Huber's converted neutrino spectra from the ILL measured electron spectra.

The validation of the MCNPX/CINDER90 methodologies for reactor core load management has been performed on extensive verifications with experimental data and cross-code comparison. It was concluded that the developed by the BR2 reactor team MCNP methodologies are capable of accurate calculation of neutron & gamma fluxes, power & fission rates distributions, fuel burn-up & isotopic fuel densities.

The next step will be to evaluate the antineutrino spectra using the summation method with pure MURE simulation, which is the most accurate method to account for "off-equilibrium effects" due to the build-up of long lived fission products, and to neutron captures during the operation cycle.

APPENDIX A: VALIDATION OF THE MCNP METHODOLOGY

For the following cycles, the reactivity evolution curves have to be interpreted taking into account some additional information:

- cycle 01/2014 depicted in Figure A.3 was a two-part cycle, whereby in the second part an unanticipated scram occurred which necessitated a partial unloading of the iridium targets, hence the reactivity jump that can be observed,
- cycle 04/2014 depicted in Figure A.3 started at a very high height of the control rods. As a result, the determination of the control rod bank reactivity worth by period measurements had a large degree of uncertainty, which resulted in an overestimated value (18.37$) of the control rod bank reactivity worth. This was the cause for non-adequate values for the measured reactivities which are based on the measured control rod bank reactivity worth.

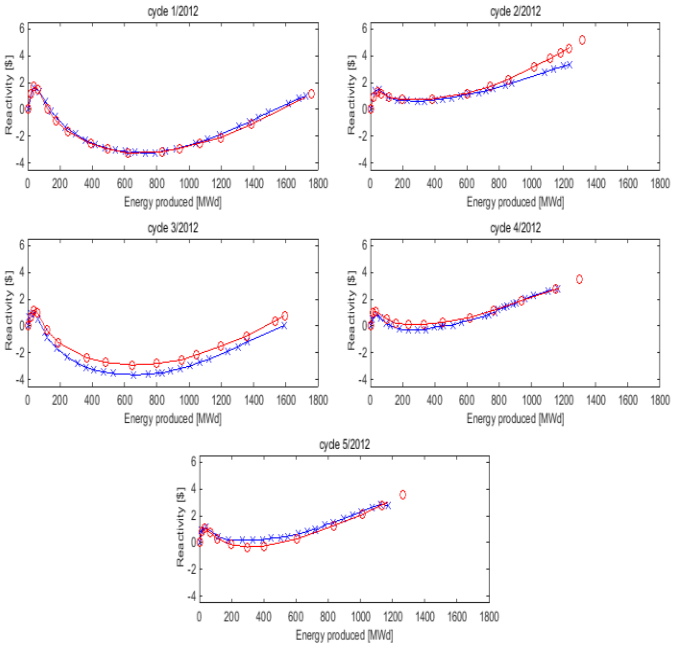

Figure A.1. Evolution of the reactivity of the BR2 reactor as a function of produced energy for the cycles of the year 2012: as measured (blue), as predicted by the MCNP based simulations (red).

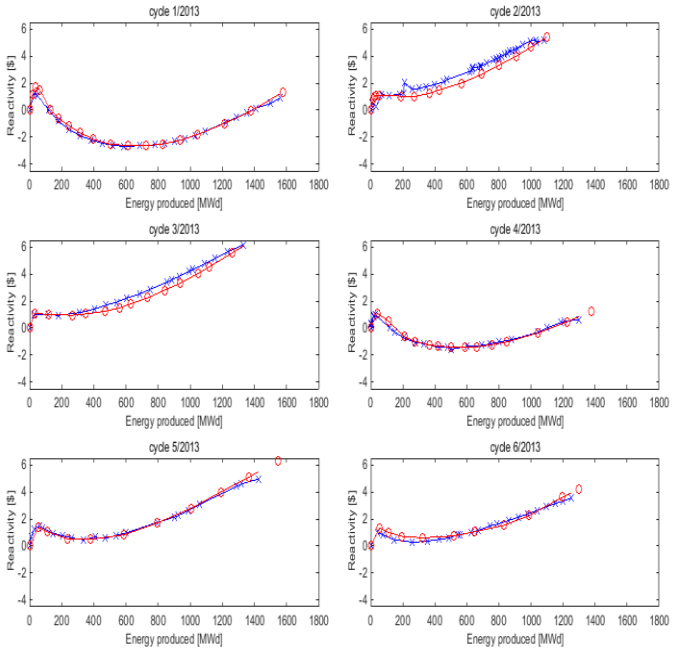

Figure A.2. Evolution of the reactivity of the BR2 reactor as a function of produced energy for the cycles of the year 2013: as measured (blue), as predicted by the MCNP based simulations (red).

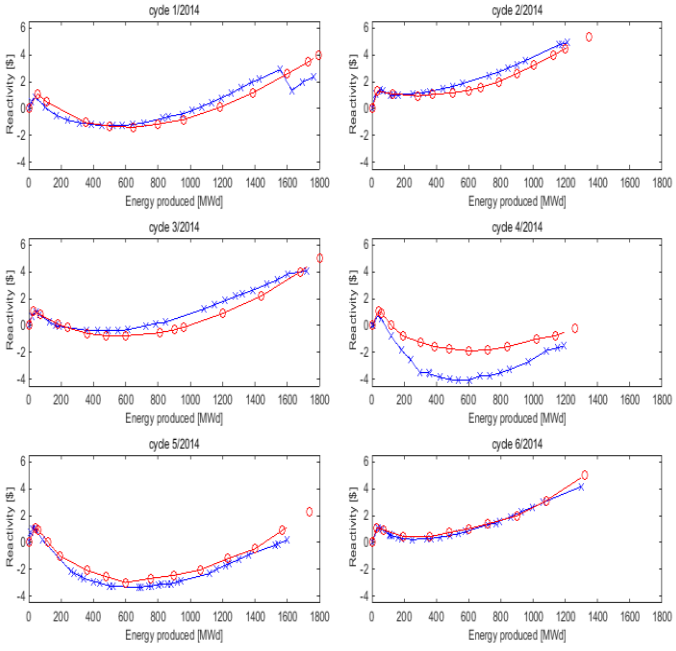

Figure A.3. Evolution of the reactivity of the BR2 reactor as a function of produced energy for the cycles of the year 2014: as measured (blue), as predicted by the MCNP based simulations (red).

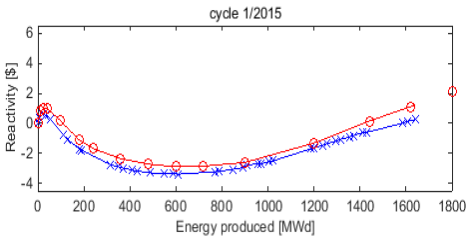

Figure A.4. Evolution of the reactivity of the BR2 reactor as a function of produced energy for the cycles of the year 2015: as measured (blue), as predicted by the MCNP based simulations (red).

Table A.1. Fission neutron flux in IPS1 (reactor channel K311) of the CALLISTO loop at the end of cycle 03/2003.A in vessel steel specimens at different axial levels, Ref. [27].

Axial position	Fission neutron	Pin				
[cm]	[n/(cm²·s)]	A	C	E	G	I
-30 – -27	measured	$9.22 \times 10^{+12}$	$8.77 \times 10^{+12}$	$7.15 \times 10^{+12}$		
	MCNP	$9.20 \times 10^{+12}$	$8.92 \times 10^{+12}$	$7.30 \times 10^{+12}$		
-19 – -16	measured				$7.50 \times 10^{+12}$	$7.24 \times 10^{+12}$
	MCNP				$7.10 \times 10^{+12}$	$7.35 \times 10^{+12}$
–4 – -1	measured	$1.16 \times 10^{+13}$	$1.16 \times 10^{+13}$	$9.51 \times 10^{+12}$	$7.54 \times 10^{+12}$	$7.37 \times 10^{+12}$
	MCNP	$1.29 \times 10^{+13}$	$1.12 \times 10^{+13}$	$9.00 \times 10^{+12}$	$7.10 \times 10^{+12}$	$7.33 \times 10^{+12}$
+11 – +14	measured				$5.52 \times 10^{+12}$	$5.54 \times 10^{+12}$
	MCNP				$6.00 \times 10^{+12}$	$5.94 \times 10^{+12}$
+24.4 – +27.4	measured	$5.11 \times 10^{+12}$	$5.32 \times 10^{+12}$	$4.05 \times 10^{+12}$		
	MCNP	$6.00 \times 10^{+12}$	$5.80 \times 10^{+12}$	$5.28 \times 10^{+12}$		
+22.9 – +28.9	measured			$4.05 \times 10^{+12}$		
	MCNP			$4.70 \times 10^{+12}$		

Table A.2. Fission neutron flux in IPS3 (reactor channel K311) of the CALLISTO loop at the end of cycle 03/2003.A in vessel steel specimens at different axial levels, Ref. [27].

Axial position	Fission neutron	Pin				
[cm]	[n/(cm²·s)]	A	C	E	G	I
-30 – -27	measured	$5.33 \times 10^{+12}$	$8.25 \times 10^{+12}$	6.77 × 10+12		
	MCNP	$7.50 \times 10^{+12}$	7.92 × 10+12	6.90 × 10+12		
-19 – -16	measured				7.12 × 10+12	7.22 × 10+12
	MCNP				6.90 × 10+12	7.35 × 10+12
–4 – -1	measured	$1.08 \times 10^{+13}$	1.10 × 10+13	8.55 × 10+12	7.26 × 10+12	7.32 × 10+12
	MCNP	$1.07\times 10^{+13}$	1.19 × 10+13	9.03 × 10+12	8.14 × 10+12	7.30 × 10+12
+11 – +14	measured				5.33 × 10+12	5.37 × 10+12
	MCNP				6.00 × 10+12	6.17 × 10+12
+24.4 – +27.4	measured	$4.75 \times 10^{+12}$	5.07 × 10+12	3.79 × 10+12		
	MCNP	$4.45 \times 10^{+12}$	5.50 × 10+12	4.00 × 10+12		

APPENDIX B: DISTRIBUTION OF THE GAMMA HEATING IN THE BR2 REACTOR

Table B.I. Gamma heating balance (MW) in BR2. The letters denote the different channels in the BR2 reactor (see Fig. 12). The calculations are performed by MCNP for total thermal power of the reactor BR2, P = 56 MW.

Geometry Part of BR2	$Q_\gamma^{\text{prompt+captured}}$	$Q_\gamma^{\text{delayed}}$	$Q_\gamma^{\text{pr+cap+del}}$
Channel H1 (Be-reflector)	0.151	0.071	0.222
H2+H3+H4+H5 (Be-reflector)	0.206	0.075	0.281
A0 around H1 (Be-reflector)	0.140	0.070	0.210
A,B channels (12 FE)	0.881	0.635	1.516
C,D channels (11 FE + 6 CR)	1.088	0.625	1.713
E,F,G channels (9 FE+Be-refl.)	0.567	0.327	0.894
H,K channels (Be-reflector)	0.211	0.084	0.295
L,N,P,S,T chan. (Be-reflector)	0.184	0.061	0.245
Al vessel & Al shroud	0.103	0.029	0.132
Light water tank	0.284	0.073	0.357
TOTAL	3.815	2.050	5.865

NOMENCLATURE

BOC – Beginning Of Cycle
CALLISTO – PWR loop in BR2, which occupied 3 channels: D180, K49 and K311 used for various materials testing (now removed in the 4th Be-matrix)
chan. – channel
cap. – capture γ – ray
CR – Control Rod
del. – delayed γ – ray
EOC – End Of Cycle
FE – Fuel Element
FIMA – Fissions per Initial Metal Atom
GERONIMO – fuel irradiation program for testing of MOX fuel rods in the BR2 reactor
H1 – beryllium channel (D=200 mm) in the reactor core center of BR2
H1/C – Central channel (D=84 mm) in H1 channel
HEU – High Enriched Uranium
IBD – Inverse Beta Decay
IPS1 – In-Pile-Section in channel K49
IPS3 – In-Pile-Section in channel K311
MOC – Middle Of Cycle
MOX – Mixed Oxide Fuel
MURE – MCNP Utility for Reactor Evolution
pr. – prompt γ – ray
PRF – Primary Water Cooled Device for Reloadable Fissile Targets
PWC/CCD – Pressurized Water Capsule/Cycling and Calibration Device
refl. – reflector
SoLid – short baseline experiment at close distance from the SCK•CEN BR2 reactor using next generation detector technology for search of new antineutrino oscillations.
SCK•CEN – Belgian Nuclear Research Center
SUBATECH – research laboratory, Ecole des Mines de Nantes
SM1 – first module of the SoLid detector
β^- - beta minus emitter/decay
e^+ - positron
n - neutron
p - proton
$\overline{\nu_e}$ - electron antineutrino
ρ - reactivity
$\Delta\rho$ - reactivity difference

REFERENCES

1. A. VACHERET et al., SoLid experiment proposal to the Institute Laue-Langevin PAC (2013).
2. L. A. MIKAELIAN, Proc. Int. Conf. Neutrino-77, Vol. 2, 383 (1978).
3. V.A. KOROVKIN et al., At. Energy 65, 712 (1988).
4. K. N. Abazajian et al., "Light Sterile neutrino: a white paper", arXiv:1204.5379.
5. V.M. BUI, L. GIOT, M. FALLOT et al.,"Antineutrino emission and gamma background characteristics from a thermal research reactor", February 2016, arXiv:1602.07522 and references therein.
6. MCNPX, Version 2.7.0, LANL, LA-UR-11-02295. April, 2011.
7. MCNP6, Version 6.1.1beta, LANL, LA-CP-14-00745, Rev. 0, June, 2014.
8. S. KALCHEVA, E. KOONEN, "Application of MCNPX 2.7.D for Reactor Core Management at the Research Reactor BR2", *M&C 2011*. Rio de Janeiro, RJ, Brazil, May 8-12, 2011, American Nuclear Society (2011) (CD-ROM).
9. S. KALCHEVA, E. KOONEN, "Automatic Whole Core Depletion & Criticality Calculations by MCNPX 2.7.0", *PHYSOR 2012*. Knoxville, Tennessee, USA, April 15-20, 2012, American Nuclear Society (2012) (CD-ROM).
10. Python Language Reference, version 3.4. Available at http://www.python.org.

11. M. FALLOT et al., "New Antineutrino Energy Spectra Predictions from the Summation of Beta Decay Branches of the Fission Products", *Phys. Rev. Lett. 109*, 202504 (2012) and references therein.
12. Th. A. MUELLER, D. LHUILLIER, M. FALLOT et al.,"Improved Predictions of reactor Antineutrino Spectra", *Phys. Rev C83*, 054615 (2011).
13. P. HUBER, "Determination of antineutrino spectra from nuclear reactors", *Phys. Rev. C84*, 024617 (2011) and references therein.
14. P. VOGEL, "Conversion of electron spectrum associated with fission into the antineutrino spectrum", *Phys. Rev. C76*, 025504 (2007).
15. K. SCHRECKENBACH, H. R. FAUST, F. VON FEILITZSCH, A. A. HAHN, K. HAWERKAMP, and J. L. VUILLEUMIER, *Phys. Lett. 99B*, 251 (1981).
16. K. SCHRECKENBACH, G. COLVIN, W. GELLETLY, and F. VON FEILITZSCH, *Phys. Lett. 160B*, 325 (1985).
17. F. VON FEILITZSCH, A. A. HAHN, and K. SCHRECKENBACH, Phys. Lett. 118B, 162 (1982).
18. A. A. HAHN, K. SCHRECKENBACH, W. GELLETLY, F. VON FEILITZSCH, G. COLVIN, and B. KRUSCHE, *Phys. Lett. B 218*, 365 (1989).
19. A. ONILLON, Prediction of the Reactor Fission Rates and the Estimation of the Associated Uncertainties in the Frame of the Double Chooz Experiment, PhD Thesis, Ecole des Mines de Nantes (2014).
20. MURE, MCNP utility for reactor evolution (2009), O. Meplan. Tech. Rep. LPSC 0912 and IPNO-09-01 (2009). URL http://www.nea.fr/tools/abstract/detail/nea-1845.
21. T. SHIBA et al., "Reactor Simulations for Safeguards with the MCNP Utility for Reactor Evolution Code", *Symposium on International Safeguards*, October 2014, IAEAheadquarters, Vienna, (Austria), IAEA-CN-220/219 and references therein.
22. S. KALCHEVA, E. KOONEN, V. KUZMINOV, G. VAN DEN BRANDEN, MCNPX 2.7.0 Licensing Package BR2: Licensing File for MCNPX 2.7.0 Methodologies Applied for Reactor Core Management at BR2, SCK•CEN-R-5188, June 2011.
23. L. VERMEEREN, J. DEKEYSER, PH. GOUAT, S. KALCHEVA, E. KOONEN, V. KUZMINOV, A. VERWIMP, M. WEBER, Qualification of the on-line power determination of fuel elements in irradiation devices in the BR2 reactor, SCK•CEN-BLG-1006, January 2005.
24. S. KALCHEVA, PH. GOUAT, Evaluation of 3-D Energy Distribution in a PWC/CCD Device Combining Thermal Balance Methods with MCNP&ORIGEN-S Calculation Model, *Proceedings of the 9th Int. Topical Meeting on Research Reactor Fuel Management RRFM2005* (p. 211–217), Budapest, Hungary, April 2005.
25. S. KALCHEVA, G. VAN DEN BRANDEN, E. KOONEN, Reactivity Performances of Two Prototypes HEU Fuel Elements with Cadmium Wires Irradiated in the BR2 Reactor, *Proceedings of RRFM2012* (p. 196–208), Prague, Czech Republic, March 2012.
26. V. KUZMINOV, E. KOONEN, B. PONSARD, Monte Carlo Simulation of Irradiation of MTR Fuel Plates in the BR2 Reactor using a full-scale 3-D Model with Inclined Channels, *Proceedings of the 6th Int. Topical Meeting on Research Reactor Fuel Management RRFM2002* (p. 206–210), Ghent, Belgium, March 2002.
27. S. KALCHEVA, "MCNP Calculations of Neutron Fluxes for Project TANGO", Restricted Contract Report, SCK•CEN-R-3827, February, 2004.
28. A. STANKOVSKIY, G. VAN DEN EYNDE, "ALEPH 2.1: A Monte Carlo Burn-up Code", SCK•CEN-R-5267.
29. S. KALCHEVA et al., *Nucl. Tech., Vol.158*, 36 (2005).